

2D-3D Geometric Fusion Network using Multi-Neighbourhood Graph Convolution for RGB-D Indoor Scene Classification[☆]

Albert Mosella-Montoro^{a,*}, Javier Ruiz-Hidalgo^a

^a*Image Processing Group - Department of Signal Theory and Communications, Universitat Politcnica de Catalunya, Barcelona, Spain*

Abstract

Multi-modal fusion has been proved to help enhance the performance of scene classification tasks. This paper presents a 2D-3D fusion stage that combines 3D Geometric features with 2D Texture features obtained by 2D Convolutional Neural Networks. To get a robust 3D Geometric embedding, a network that uses two novel layers is proposed. The first layer, Multi-Neighbourhood Graph Convolution, aims to learn a more robust geometric descriptor of the scene combining two different neighbourhoods: one in the Euclidean space and the other in the Feature space. The second proposed layer, Nearest Voxel Pooling, improves the performance of the well-known Voxel Pooling. Experimental results, using NYU-Depth-v2 and SUN RGB-D datasets, show that the proposed method outperforms the current state-of-the-art in RGB-D indoor scene classification tasks.

Keywords: Convolutional Graph Neural Network, Multi-modal fusion, Multi-Neighborhood Graph Neural Network, Indoor scene classification, RGB-D

[☆]Funding: This work was supported by Secretary of Universities and Research of the Generalitat de Catalunya and the European Social Fund via a PhD grant (FI2018) in the framework of project TEC2016-75976-R, financed by the Ministerio de Economia, Industria y Competitividad and the European Regional Development Fund (ERDF).

*Corresponding author

Email addresses: albert.mosella@upc.edu (Albert Mosella-Montoro), j.ruiz@upc.edu (Javier Ruiz-Hidalgo)

1. Introduction

The Scene Classification task aims to annotate a sensor capture with a scene class, such as beach, furniture store, bedroom, among others. Due to the rising interest in domotics, surveillance, and robotics applications, the RGB-D indoor scene classification task has received more attention from academia and industry. Despite the advance of the techniques applied to the recognition of object-centric data, these techniques do not have the same performance on indoor scene classification. The main reason is that an indoor scene is formed by a relationship of multiple objects which classes are open-set. For instance, recognizing a bed and a chair alone can not classify the scene as a bedroom, because these objects can exist in other scene categories such as a furniture store. Furthermore, there is a data scarcity problem as existing RGB-D datasets are still order-of-magnitude smaller than their respective 2D datasets. Other important challenges that need to be faced in this task are the considerable variation in lights, shapes, and layouts for each class of scene. Most of these challenges have been proved very difficult to solve without the 3D information that is lost in the 2D image capturing. For this reason, the use of stereo-camera configurations, RGB-D sensors, or lidars is recommended. The structure of data captured by these sensors can be organized, like captures done by a Microsoft Kinect sensor, or unorganized, like the information provided by a lidar.

Convolutional Neural Networks (CNN's) are extensively used in computer vision in a wide variety of tasks such as image classification, super-resolution, object detection, and segmentation. Nevertheless, the convolution operation is defined in a lattice structure. That means, data that is not located in a lattice structure can not be processed by CNN's directly as it is the case of unorganized 3D point clouds. This limitation can be solved with Geometric Learning, a set of techniques that convert this data on an artificial lattice structure, such as the methods that use voxels to allow the application of 3D CNN's. Another way to handle this kind of data is by using Graph Convolutional Neural Networks (GCNN's). These networks convert a 3D point cloud to a graph and create an

artificial lattice structure through the edges of the graph.

This paper proposes a new methodology that fuses the geometric information of 3D point clouds obtained by the novel Multi-Neighbourhood Graph Convolution network and the 2D Texture information obtained by a conventional CNN such as Resnet architecture [1]. The proposed 2D-3D Fusion stage does this combination taking into account the intrinsic geometric context information provided by RGB-D sensors. The point cloud is obtained using the intrinsic parameters of the camera and the depth capture.

The main contributions of this paper can be summarized as:

- The proposal of the Multi-Neighbourhood Graph Convolution operation, that outperforms previous methods to obtain geometric information. This convolution takes into consideration the neighbours of the center point in Feature and Euclidean spaces.
- The Nearest Voxel Pooling algorithm consists of an improved version of the current Voxel Pooling algorithm [2], which mitigates the noise introduced by sensors.
- The fusion of 2D-3D and multi-modal features through the proposed 2D-3D Fusion stage. Using geometric proximity allows the network to exploit the benefits of 2D and 3D Networks simultaneously.

2. Related work

2.1. Geometric Learning

Geometric deep learning consists of a set of emerging techniques attempting to generalize structured deep neural models to non-Euclidean domains or non-structured data such as 3D point clouds. One of the first approaches to process 3D point clouds was the use of Multi-view based techniques [3, 4, 5, 6]. These sets of techniques represent a 3D space as a collection of 2D views where the structured deep neural models can be used. However, due to the fact that the 2D view has lost the 3D spatial relation, the geometric information obtained

is limited. To work directly in a 3D point cloud different kinds of data structure and network architectures have been proposed, such as voxel grid networks [7, 8, 9, 10, 11] and octree networks [12]. Furthermore, a new strategy to work with 3D point clouds and meshes is to represent these data as a graph, where edges are used to create a kind of lattice structure. Two main strategies can be followed to work with these graphs. *Graph Neural Networks* [13] [14] where the graph is processed applying a neural network recurrently to every node of the graph, and *Graph Convolutional Networks* [15], where a generalization for a graph data of the discrete convolution is proposed. An improvement of this generalization was proposed by *Wang et al.* [16] that proposes the Dynamic Edge Convolution operation. This operation computes each node’s feature doing an aggregation over the output of a multi-layer perceptron (MLP) that was applied to the neighbourhood. Following this line of research, *Verma et al.* [17] propose *FeaStNet*. Where the graph-convolution operator consists in establishing correspondences between filter weights and graph neighbourhoods with arbitrary connectivity was proposed. More recently, *Mosella-Montoro et al.* [18] presents the Attention Graph Convolution, which creates an attention weight based on the geometrical attributes of the edges.

2.2. Scene classification

Earlier works of scene classification using RGB information made use of handcrafted features [19, 20] to obtain the properties of the scene. Nowadays, with the emergence of deep learning techniques and new datasets, better features can be obtained. Places-CNN [21] is a vast dataset of RGB indoor-scene captures that was used to train different standard architectures, such as VGG [22] and Resnet [1], providing one of the most successfully deep feature learning models for RGB data. Instead of finding deep features to describe the scene, *George et al.* [23] propose to capture the occurrence statistics of objects in scenes, capturing the informativeness of each detected object for each scene. As noted in the introduction, another way to tackle the Scene Classification problem is by using depth information. *Li et al.* [24] propose a novel discriminative fusion

network which can learn correlative and distinctive features of each modality. *Cai et al.* [25] propose a multi-modal CNN that captures locals structures from the RGB-D scene images and learn a fusion strategy. Similarly, MAPNet [26] presents two attentive pooling blocks to aggregate semantic cues within and between features modalities. More recently, TRecgNet [27] tackles the RGB-D Scene Recognition problem as a combination of a translate and classification problem. Their work proposes to train simultaneously a classifier network that classifies the scene and a translation network, that predicts the depth from RGB and the RGB from the depth. Training the network in a multitask manner helps the network learn more generic features that yield an increment of performance. However, these methods use a 2D CNN to obtain geometric information that introduces possible errors due to missing local geometric context that the projection to a 2D world can produce. To solve that, in [18], authors propose to extract the geometric information directly on the 3D world. The network exploits the intrinsic geometric context inside a 3D space using as input 3D point clouds obtained from RGB-D captures. However, the nodes of the graph do not have any colour or geometry information. In this work, the performance of the extraction of geometric feature is increased using the proposed Multi-neighborhood Graph Convolution. This convolution fuses two different neighbourhoods, one in the Euclidean space and the other in the Feature space. That helps to improve the quality of the extracted features. More details are given in Sec. 3.

3. Methodology

3.1. Overview of framework

The framework proposed is illustrated in Fig. 1. As it is depicted, the 3D Geometric and 2D Texture features are firstly extracted. The input of the 3D Geometric branch is a 3D point cloud. Each node of the input point cloud encodes the depth information using the HHA encoding [28], that has been proved to obtain better results in different works [26, 27]. HHA encodes the depth into a 0 to 255 range with three channels. Each channel represents horizontal dis-

parity, height above the ground, and the angle the points local normal surface makes with the inferred gravity direction. The input of the 2D Texture branch is a standard 2D image corresponding to the same capture. After the corresponding branches, both extracted features are fused using the 2D-3D Fusion stage, and the result of this stage is used by the Classification network to predict the corresponding scene class.

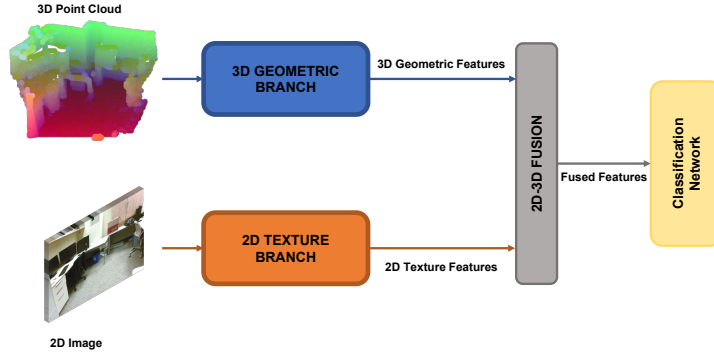


Figure 1: Illustration of the framework of 2D-3D Geometric Fusion network using Multi-Neighbourhood Graph Convolution.

The 2D Texture branch uses as a backbone the well-known architecture ResNet-18 [1] as is depicted in Fig. 2. The classification stage is removed, and the output of the last Residual block corresponds to the 2D Texture features used for the Fusion stage. This branch aims to exploit the power of already proven CNN’s to obtain texture information that will be aggregated to the geometric information obtained by the 3D Geometric branch.

ResNet-18 is composed of the combination of residual blocks, convolutional layers, and poolings. A Residual Block is a stack of two convolutional layers (F) with a shortcut that contains a projection function (P), as is shown in Fig. 3. The aim of using a projection function is to add the input to the output when both have a different shape. In that case, the projection function used by ResNet-18 is a convolutional layer with a kernel size of 1x1 without bias. When both shapes are the same, the projection function is the identity matrix. That kind of block helps obtain higher accuracy in centric-image classification, reduces

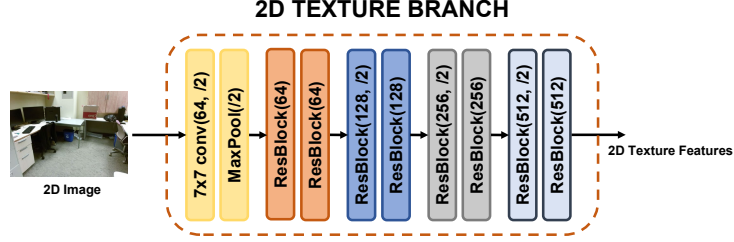


Figure 2: 2D Texture branch architecture, where $/2$ means that the stride has a value of 2 in order to downsampling the image by a factor of 2.

the effect of the vanishing gradient problem, and accelerates the convergence of the deep networks.

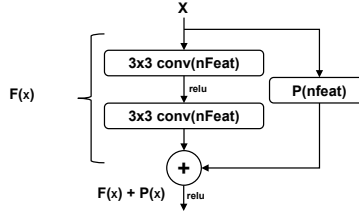


Figure 3: Illustration of a Residual Block.

The 3D Geometric branch is composed of two novel layers named Multi-Neighbourhood Graph Convolution (MUNEGC) and Nearest Voxel Pooling(NVP), both layers are explained in detail on Secs. 3.1.1 and 3.1.2 respectively. The architecture of the 3D Geometric branch is also inspired by ResNet, where MUNEGC replaces the convolution layers and residual blocks, and the Nearest Voxel Pooling layer replaces the 2D pooling layers. ResNet-18 makes use of the strides of the convolution to do the downsampling. However, that behaviour is not possible to be reproduced with the proposed Graph Convolution. For this reason, to do this downsampling, each MUNEGC layer is followed by a Nearest Voxel Pooling. In Fig. 4 the architecture used for the 3D-geometric branch is depicted.

The 2D-3D Fusion stage takes the features generated by the previously commented 2D and 3D branches and fuses them. Notice that the output resolution

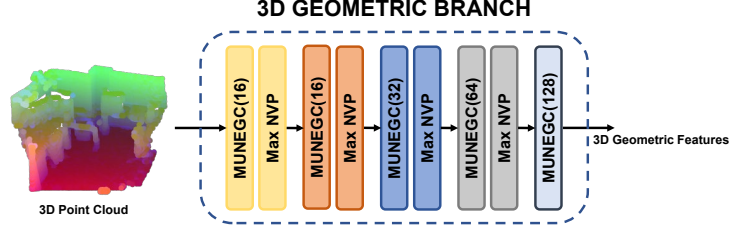


Figure 4: 3D Geometric branch architecture.

and sampling of both branches are different. The reason is that pooling layers of both branches work on different spaces (2D and 3D). As a result, the final number of points and their positions are different. The proposed 2D-3D Fusion stage can handle that behaviour and generate a new set of combined features. This stage will be explained in detail in Sec. 3.2. The new set of features is fed to the Classification network. The classification architecture, as depicted in Fig. 5, is composed of a global average pooling and an $FC(nClasses)$ layer, where FC is a Fully Connected layer and $nClasses$ is the number of scenes that the network should predict.



Figure 5: Illustration of the Classification network.

3.1.1. Multi-Neighbourhood Graph Convolution (MUNEGC)

Multi-Neighbourhood Graph Convolution (MUNEGC) is a graph operation that estimates the new feature of each node using two different neighbourhoods, as is depicted in Fig. 6.

The first step that this convolution does is to create two neighbourhoods. In this step, the edges and its attributes are generated for each neighbourhood. The difference between both generated neighbourhoods is that in the Euclidean Neighbourhood, the Euclidean position is used to find the corresponding edges. In contrast, in the Feature Neighbourhood, the node features are used to find the edges. The use of two different neighbourhoods helps to learn a more robust

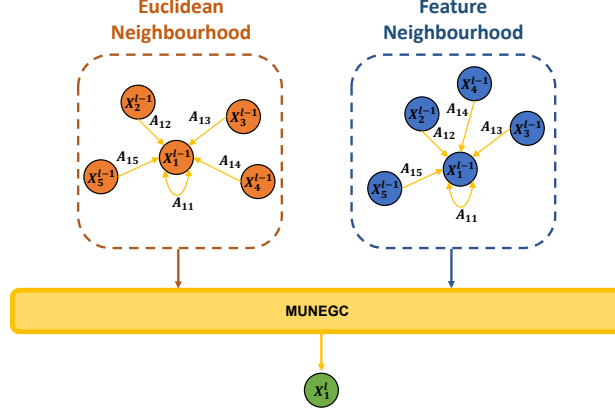


Figure 6: Multi-Neighbourhood Graph Convolution. Where X_i is the node feature vector i , A_{ij} is the edge's attribute vector of nodes ij , and l corresponds to a layer index in a feed-forward neural network.

node feature that considers the characteristics of the regions that have similar characteristics, and the regions that are close to the node.

The edges can be generated following a kNN-policy or a Radius-policy. Whereas in the Euclidean Neighbourhood, the Radius-policy has a geometric meaning and is intuitive to choose. In the Feature Neighbourhood, the meaning of this radius is unclear and is not recommended to use it due to the complexity of its selection. The reason is that the feature space that is going to be used is unknown because it will change on each iteration of the training phase. When both neighbourhoods are defined, the next step is to apply the graph convolution operation. MUNEGC makes use of an extended version of the Attention Graph Convolution (AGC) [18]. Fig. 7 depicts the AGC operation over a node N_1 of an input neighbourhood.

AGC is a graph convolution that performs the convolution over local graph neighbourhoods exploiting the edges and its attributes. These edges are used to create an artificial lattice structure which is needed to apply a convolution. Furthermore, the attributes of the edges are used to estimate the weights of the filter that will be used in each neighbourhood. The generation of weights are based on a *Dynamic Filter Network* [29] which can be implemented with

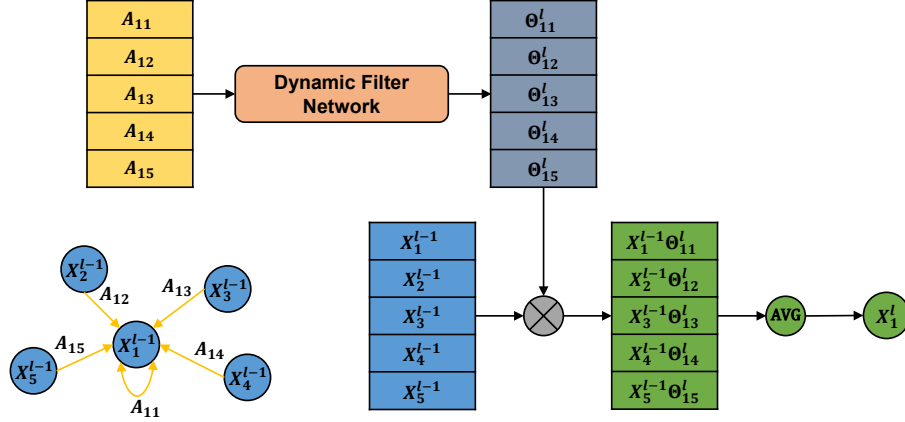


Figure 7: AGC applied to a local neighbourhood. Where X_i is the node feature vector i , A_{ij} is the edge’s attribute vector of nodes ij . Θ_{ij} are the weights generated by the Dynamic Filter Network, l corresponds to a layer index in a feed-forward neural network.

any differential architecture. In the case of AGC, the Dynamic Filter network is implemented using $FC(x)$ layers, where FC is a fully connected layer and x the number of output features of the layers. The Dynamic Filter Network is in charge of the attention mechanism. It generates weights conditioned by the attributes of the edges of the neighbourhood. In AGC, the proposal was to use positional offsets as attributes such as Euclidean or Spherical offsets that means, Dynamic Filter Network will pay attention to the nodes depending on their proximity information. AGC is formalized in Eq. (1) where X is the node feature vector, N the set of neighbourhoods, W represents the Dynamic Filter Network, A represents the edge attributes and b a learnable bias of the layer. Index i indicates the current node to evaluate, l corresponds to a layer index in a feed-forward neural network and j the neighbours of the node i .

$$X_i^l = \frac{1}{|N(i)|} \sum_{j \in N(i)} W^l(A_{ij}) X_j^{l-1} + b^l \quad (1)$$

MUNEGC proposes two extensions to the vanilla AGC. The first one is to apply a \tanh activation layer to the weights generated by the Dynamic Filter Network to prevent the network from predicting large weights that can provoke

unstable learning. The second one is to add a node feature offset as an attribute of the edge. In MUNEGC, each edge’s attribute can be seen as the combination of positional and feature offsets of the node. That enforces MUNEGC to estimate an attention weight depending on the proximity of the node and its similarity. It is essential to know that this definition of the edge’s attributes applies to both neighbourhoods. Notice that in the Feature Neighbourhood, the features are used to estimate the neighbours of a point. In this specific case, it is important to have the positional offset of each neighbour. It does not have the same influence a neighbour with similar characteristics that is near to the point than a neighbour that is far with similar characteristics. For this reason, the Dynamic Filter Network needs in both cases, the positional and the feature offsets, to properly learn the characteristics of each neighbourhood. Eq. 2 defines the edge attribute vector where S_{ij} is the positional offset and K_{ij} is the offset between features X_i and X_j .

$$A_{ij} = \{S_{ij}, K_{ij}\} \quad (2)$$

Furthermore, as mentioned before, to calculate the new feature of a node, MUNEGC makes use of two neighbourhoods. Eqs. 3 and 4 formalize the MUNEGC. Where index e indicates Euclidean Neighbourhood and f corresponds to the Feature Neighbourhood. The filter used on the Euclidean and Feature Neighbourhood has the same size. By definition, if a MUNEGC of M features is requested, the filter applied to each neighbourhood will also output M features, and these features should be aggregated. $Aggr\{\cdot\}$ represents the maximum or average aggregation of features. The result of this operation must be M features.

$$F(A_{ij}) = \tanh(W(A_{ij})) \quad (3)$$

$$X_i^l = \text{Aggr} \left\{ \frac{1}{|N_e(i)|} \sum_{j \in N_e(i)} F_e^l(A_{ij}) X_j^{l-1} + b_e^l, \right. \\ \left. \frac{1}{|N_f(i)|} \sum_{j \in N_f(i)} F_f^l(A_{ij}) X_j^{l-1} + b_f^l \right\} \quad (4)$$

3.1.2. Nearest Voxel Pooling (NVP)

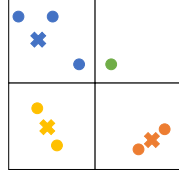
The Nearest Voxel Pooling (NVP) layer is based on the Voxel Pooling (VP) algorithm [2]. The VP algorithm consists in creating voxels of resolution r_p^l over the point cloud and replacing all points inside the voxel with their centroid. The centroid’s feature is the average or the maximum of the features of the points inside the voxel. However, VP can introduce some errors when the points inside of two different voxels are closer than its respective voxel’s centroid.

The proposed NVP layer reformulates the VP algorithm to solve the issue explained before. In Fig. 8, a comparison of the performance of both algorithms is shown. The algorithm behind the NVP follows these steps:

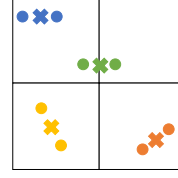
1. Create voxels of resolution r_p^l .
2. Estimate the centroid’s position doing the mean of the position of the nodes inside the voxel.
3. For each point of the point cloud, find the closest centroid and group the points that have the same closest centroid.
4. Remove empty voxels and centroids that does not have any point assigned.
5. For each group of points estimate the superpoint’s position, doing the mean of the positions of the points inside the group.
6. Superpoint’s feature is the average or the maximum of the features of the points that belong to the superpoint’s group.

3.2. 2D-3D Fusion stage

The 2D-3D Fusion stage is defined to fuse different sets of multi-modal features. This stage will be used in this work to make the fusion of the 3D Geometric and 2D Texture features. In Fig. 9 is depicted the architecture proposed.



(a) Voxel pooling example.



(b) Nearest voxel pooling example.

Figure 8: Comparison of (a) Voxel pooling and (b) Nearest voxel pooling. Crosses represent the new superpoint and the dots the original points. Voxels where there is only one point the superpoint, and the original point is represented as a dot.

This stage’s first step is to project the 2D Texture features into the 3D space using the camera parameters, allowing to exploit the geometric information inside the 3D space to do the fusion. The next step is to apply a Projection function (P) in charge of projecting the 3D Geometric and 2D Texture features to a different feature space. The motivation of this P is that each kind of input features can have different dimensions. To solve that, P projects each kind of input features to another feature space that have the same dimensionality. Notice that each kind of feature has its own P , P_g for projecting 3D Geometric features and P_t for projecting 2D Texture features. Both are defined as a convolutional layer with a kernel size of 1x1 without bias.

The projected features are fused using a version of the previously explained Nearest Voxel Pooling algorithm, which is used only to create groups of points. Each group of points contains the projected version of the 2D Texture and 3D Geometric features, as is shown in Fig. 10. For each group of points, a superpoint is generated. The position of this superpoint is the average of the positions of the points inside the same group. To estimate the fused feature of each superpoint, it is required to follow two steps. First, the average of the same kind of features inside the same group is calculated. Then, the resulting averages are concatenated, generating the fused feature that it will contain each superpoint. If there is only one kind of feature in one group, the other positions of the fused vector are going to be filled with 1.

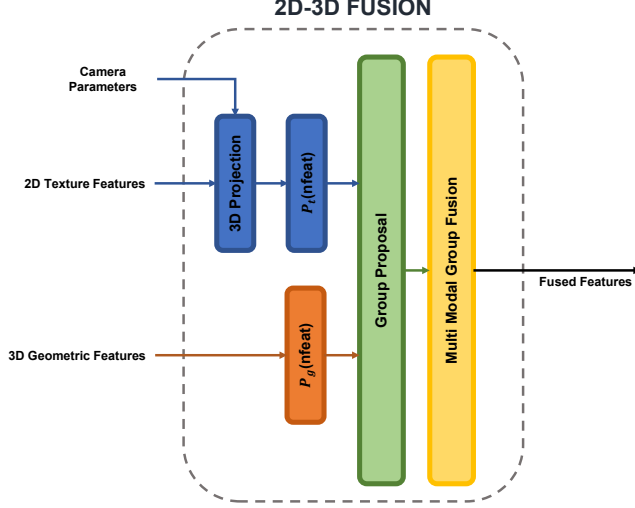


Figure 9: 2D-3D fusion stage architecture where P_g is the projection function of the 3D Geometric features, P_t is the projection function of the 2D Texture features.

Eq. 5 defines this fusion. Where X is a feature vector, P_g is the projection function of the 3D Geometric features, P_t is the projection function of the 2D Texture features, N is the set of points inside the same group. Index i indicates the current group to evaluate, g indicates that belongs to the 3D Geometric features group, and t indicates that belongs to the 2D Texture features group.

$$X_i = \text{Concat} \left\{ \frac{1}{|N_g(i)|} \sum_{X \in N_g(i)} P_g(X), \frac{1}{|N_t(i)|} \sum_{X \in N_t(i)} P_t(X) \right\} \quad (5)$$

4. Experiments

4.1. Datasets

The SUN RGB-D dataset [30] includes 10335 RGB-D captures. The dataset was captured from different RGB-D sensors including Asus Xtion, RealSense, Kinect v1 and Kinect v2. Following the settings proposed by the authors, classes with less than 80 samples are discarded. In the end, 9504 captures

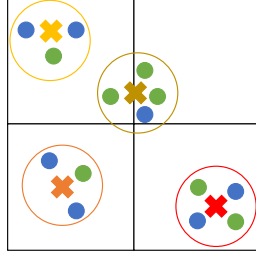


Figure 10: Example of the group’s creation for the 2D-3D fusion stage. Each dot color represents a different kind of feature. Each circle represents a different group and the crosses represent the centroid of each group.

remain with 19 different classes. These captures were divided in 4845 for training and 4659 for testing using the official split.

The NYU Depth Dataset V2 (NYUV2)[31] contains 1449 RGB-D captures with 27 classes. Following the standard configuration, the categories are grouped into 10, including 9 most common categories and the *Other* category representing the rest. Moreover, the standard split is followed, where 795 captures are used in the train split and 654 for testing.

4.2. Training details

The proposed approach is implemented on Pytorch [32] and Pytorch Geometric [33]. Due to GPU memory constraints, each branch of the network is trained in an isolated manner adding an independent classification network for each branch. This Classification network is initialized randomly and the bias of the fully connected layer is initialized as $b = -\log((1 - \pi)/\pi)$ where π is defined as $\pi = 1/C$ where C is the number of classes. This initialization aims to avoid the possible training instability that bias $b = 0$ could cause at the beginning of the training as it is explained by *Cui et al.* [34].

Both datasets used in this paper are characterized to have an unbalanced number of images for each category. This work uses a weighted cross-entropy (WCE) loss to handle the imbalance issue during training in all branches. Specif-

ically, the following re-scaling strategy is used:

$$WCE(x, y) = w[y] \left(-x[y] + \log \left(\sum_j e^{x[j]} \right) \right) \quad (6)$$

Where x is the output vector of the network, y is the ground truth label, and w is the weight vector that contains a different weight for each class. The $w(y)$ is computed using the inverse class frequency, $f(y)$, as described in Eq. 7.

$$w(y) = 1/f(y) \quad (7)$$

Furthermore, to make the total loss in the same scale when the weight is applied, $w(y)$ is normalized so that $\sum_{t=1}^C w(y) = C$ where C is the total number of classes.

The **Texture branch**, as explained in Sec. 3, uses ResNet18 as backbone. Similar to previous works [27, 26], weights are initialized using a ResNet-18 pre-trained on Places dataset [21] in the SUN RGB-D dataset. For the smaller NYUV2 dataset, ResNet-18 is initialized using the weights obtained on the training done in the SUN RGB-D dataset. In both datasets, the network is trained during 100 epochs with a batch size of 16. The optimizer used for this training is SGD with momentum. The learning rate used is 1×10^{-3} with a momentum of 0.9 and a weight decay of 1×10^{-4} . A center crop of 560×420 is applied to the RGB images of both datasets. Besides, a random horizontal flip is applied during training.

In the case of the **3D Geometric branch**, weights are initialized randomly for the SUN RGB-D dataset as there is no bigger RGB-D dataset to perform a pre-train of the network. In the case of the NYUV2 dataset, as done in the Texture branch, weights obtained on SUN RGB-D are used to initialize the branch. In both datasets, the network is trained during 200 epochs with a batch size of 32. The optimizer used for this training is the Rectified Adam(RADAM) [35], an improved version of ADAM that rectifies the variance of the adaptive learning rate. The learning rate used is 1×10^{-3} , betas (0.9, 0.999) and a weight decay of 1×10^{-4} . A dropout layer is added before the Fully Connected of

the Classification network with a probability $p = 0.2$ to be zeroed. The radius chosen for the pooling layers can be seen in Table 1. The Dynamic Filter Network configuration chosen for all MUNEGC layers is: $FC(128) - FC(d_l \cdot d_{l-1})$ where d_l is the number of output features of layer l . The average aggregation is used in MUNEGC layers. In both datasets, a 3D point cloud is obtained using the depth capture and the camera parameters. As explained on Sec. 3.1, the features of each point of the 3D point cloud are the HHA encoded version of the depth capture. The obtained 3D point cloud is converted to a graph using a kNN-policy with $k = 9$. The edges of this graph have as attributes: the Spherical offset and the Feature offset. Finally, the following techniques of online data augmentation are applied: 1) Rotation over the vertical axis randomly between $(0, 2\pi)$. 2) Mirroring over horizontal axis randomly with a probability of 0.5. 3) Random removal of points in the input 3D point cloud with a probability of 0.2. 4) A novel 3D random crop proposed in this work. This technique consists in finding a random centroid, for each axis, a random value between the maximum and minimum is chosen. A factor f is defined to specify the desired number of points inside the crop. The values of f are in the range of $0 < f < 1$. The desired number of points (dn) is defined as $dn = npoints \times f$, where $npoints$ is the number of points of the original point cloud. Finally, a radius that accomplishes the following condition $npoints_inside < dn$ is found, where $npoints_inside$ indicates the number of points inside the proposed radius. The crop is made up of the points inside the sphere defined by the radius found. In this work, the f is equal to 0.875.

Pooling Layer	Radius(meters)
PNV 1	0.05
PNV 2	0.08
PNV 3	0.12
PNV 3	0.24

Table 1: Pooling radius configuration of 3D Geometric Branch.

Finally, the **2D-3D fusion stage** and the **Classification network** are considered the last branch, and both networks are trained together. In both datasets, weights are initialized randomly. The input of this branch is the output features of both previous branches, without its corresponding classification networks as it can be seen in Fig. 1, and the camera parameters. The network is trained during 20 epochs with a batch size of 32. Rectified Adam(RADAM) [35] is used for the training with a learning rate of 1×10^{-3} , betas (0.9, 0.999) and a weight decay of 1×10^{-4} . A dropout layer is added before the Fully Connected of the classification network with a probability $p = 0.5$ to be zeroed. The radius used to fuse the features in the 2D-3D fusion stage is $r = 0.24$.

4.3. Results on SUN RGB-D dataset

4.3.1. Comparison with state-of-the-art methods

In this section, the final results of the proposed method are compared with the most recent state-of-the-art in Indoor Scene Classification. The backbone of the previous methods is more or less the same. All of them use a pre-trained 2D-CNN to obtain geometric and texture features. DF²Net [24] make use of a triplet loss to encourage the network to learn discriminative and correlative features to do a better fusion. MAPNet [26] improves the fusion stage, adding two attentive pooling blocks to aggregate semantic cues within and between features modalities. TRecNet [27] propose to use a combination of a translate and classification problem, that predicts the depth from RGB and the RGB from the depth. This approach allows TRecNet to obtain more generic features and extra data that can be used in training. The method proposed in this paper tries to improve the performance using a completely different approach. First, the geometric features are obtained in a 3D space using the proposed graph convolution MUNEGC and the pooling layer NVP, that allows the network to exploit the intrinsic geometric context inside a 3D space. The fusion strategy is tackled by the novel 2D-3D fusion stage that, using geometric proximity, allows the network to exploit the benefits of 2D and 3D Networks simultaneously. With these contributions, the proposed method improves previous state-of-the-

art methods with an increment of 1.8% in the mean accuracy, as shown in Table 2.

Method	Mean Acc.(%)
DF ² Net [24]	54.6
MAPNet [26]	56.2
TRecNet [27]	56.7
Ours	58.5

Table 2: Performance comparison with state-of-the-art methods on SUN RGB-D Dataset.

One of the disadvantages of the proposed method is the lack of large RGB-D datasets to do a proper pre-train of the 3D Geometric branch. Table 3 compares the mean accuracy using only geometric features in TRecNet, that is the best method on the current-state-of-the-art and the 3D Geometric features of the proposed framework. It shows that using pre-trained features helps TRecNet improve up to 5.4% the mean accuracy. However, the proposed 3D Geometric branch exceeds the mean accuracy of TRecNet when is initialized randomly.

Method	Initialization	Mean Acc.(%)
TRecNet [27]	Places	47.6
TRecNet [27]	Random	42.2
<u>Ours</u>	<u>Random</u>	<u>44.1</u>

Table 3: Performance comparison of geometric feature branch with state-of-the-art methods on SUN RGB-D Dataset.

4.3.2. Study of different strategies to generate the neighborhood and the attributes of the edges

In this section, different strategies to generate the neighbourhood and their respective edge attributes will be studied. All parameters and configurations explained in Sec. 4.2 are fixed. In order to generate the neighbourhoods, two

different policies can be used: kNN and Radius. However, the Radius-policy can not be applied in the Feature Neighbourhood as features are still being defined during the training phase, which difficulties the choice of a radius. For this reason, the study of the two main policies will be done in the Euclidean Neighbourhood. A radius has been chosen for each MUNEGC layer. The best radius found where: $[0.05m, 0.08m, 0.12m, 0.24m, 0.48m]$ for each corresponding MUNEGC layer. As it can be observed in Table 4, kNN-policy surpasses the mean accuracy obtained with Radius-policy in this scenario.

Method	Mean Acc.(%)
kNN-policy	44.1
Radius-policy	42.44

Table 4: Analysis of kNN and radius as edge generation policy in Euclidean Neighbourhood.

Once the neighbourhood is defined, an attribute for each edge should be assigned. In Table 5 can be seen as an analysis of different edge’s attribute on each kind of neighbourhood. The best configuration is the use of Spherical offset and Feature offset on both neighbourhoods. As can be seen, both offsets are required in both neighbourhoods, as is explained in Sect. 3.1.1.

Euclidean attributes	Feature attributes	Mean Acc. (%)
Spherical + Feature offsets	Spherical + Feature offsets	44.1
Cartesian + Feature offsets	Cartesian + Feature offsets	42.27
Spherical + L2 offsets	Spherical + L2 offsets	40.45
Spherical offset	Feature offset	40.24

Table 5: Analysis of the effectiveness of different edge attributes on each kind of neighbourhood. L2 offset is the L2 distance between the feature vector of two neighbours.

4.3.3. Analysis of the MUNEGC design

In this section, the MUNEGC design will be analyzed. As it is explained in Sec. 3.1.1 MUNEGC propose to extensions to the vanilla AGC [18]. The first one is to add a node feature offset as an attribute of the edge. The second one is to create a mechanism to prevent the prediction of large weights by the Dynamic Filter Network that can cause unstable learning. A \tanh is added as an activation layer at the end of the network. In Table 6 can be observed the influence of each one of these extensions.

layer	Spherical offset	Feature offset	tanh	Mean Acc.(%)
AGC	Yes	No	No	35.2
AGC	Yes	Yes	No	41.53
AGC	Yes	Yes	Yes	42.37
MUNEGC	Yes	Yes	Yes	44.1

Table 6: Analysis of the performance of each improvement done in MUNEGC.

Furthermore, in Table 7, the influence of the aggregation method of both neighbourhoods in MUNEGC can be seen. The average aggregation shows a better performance than the maximum aggregation.

Method	Mean Accuracy(%)
Average	44.1
Maximum	40.7

Table 7: Comparison between maximum and average aggregation in MUNEGC.

4.3.4. Analysis of the Nearest Voxel Pooling

The Nearest Voxel Pooling (NVP) is an improved version of the Voxel Pooling (VP) that solves the drawback of VP when the points inside of two different voxels are closer than its respective voxels centroid. NVP layers are replaced to

VP layers to analyze the performance of the proposed NVP in the 3D Geometric branch. Table 8 shows that the NVP is achieving better results than VP.

Method	Mean Acc.(%)
NVP	44.1
VP	42.5

Table 8: Comparison between Nearest Voxel Pooling (NVP) and Voxel Pooling (VP) algorithms.

4.4. Results on NYU depth dataset V2

The proposed frameworks are also evaluated on the NYUV2 dataset and compared with the state-of-the-art. Unlike the experiments done in SUN RGB-D dataset, in this dataset, the 3D geometric branch can be pre-trained using the weights obtained from the training on SUN RGB-D. As it can be seen in Table 9, the proposed method overcomes the state-of-the-art by 6% of mean accuracy. Experiments on NYUV2 reveals that the proposed 3D Geometric branch composed by MUNEGC and NVP has the ability to learn generalized representations that can be used to other datasets, making possible to apply transfer learning techniques as conventional 2D-CNN’s.

Method	Mean Acc.(%)
DF ² Net [24]	65.4
MAPNet [26]	67.7
TRecNet [27]	69.2
Ours	75.1

Table 9: Performance comparison with state-of-the-art methods on NYU Depth Dataset V2 Dataset.

In Table 10 it can be seen the comparison of performance between the proposed Geometric branch and TRecNet, that is the best method on the current-

state-of-the-art. As it can be seen when the proposed method is initialized randomly has better accuracy than TRecNet when this one is initialized with Places. Furthermore, the proposed method outperforms TRecNet when both are initialized with the same dataset.

Method	Initialization	Mean Acc.(%)
TRecNet [27]	Places	55.2
TRecNet [27]	SUN RGB-D	57.7
<u>Ours</u>	<u>Random</u>	<u>57.2</u>
Ours	SUN RGB-D	59.2

Table 10: Performance comparison of geometric feature branch with state-of-the-art methods on NYU Depth Dataset V2 Dataset.

5. Conclusions

This paper proposes a 2D-3D Geometric Fusion Network that exploits the intrinsic geometric information of the 3D-space to obtain geometric features and improves the fusion with the texture features. The geometric features are obtained by the 3D Geometric branch that is composed by Multi-Neighborhood Graph Convolutions (MUNEGC) and Nearest Voxel Pooling (NVP) layers and the 2D Texture features are obtained by a standard 2-CNN as it is ResNet-18. The 2D-3D fusion stage does the fusion of the 3D Geometric features and the 2D Texture features, that exploits 3D geometric proximity to fuse both features. As experiments demonstrate on SUN RGB-D and NYUV2 dataset, the proposed method outperforms state-of-the-art results validating the effectiveness of the all proposed layers and stages. One direction of the future work is to explore the possibility to transfer the knowledge obtained by a pre-trained 2D-CNN to the proposed MUNEGC network using Student-Teacher Networks.

References

- [1] K. He, X. Zhang, S. Ren, J. Sun, Deep Residual Learning for Image Recognition, in: Conference on Computer Vision and Pattern Recognition (CVPR), IEEE, 2016, pp. 770–778.
- [2] M. Simonovsky, N. Komodakis, Dynamic edge-conditioned filters in convolutional neural networks on graphs, in: Conference on Computer Vision and Pattern Recognition (CVPR), 2017, pp. 29–38.
- [3] H. Su, S. Maji, E. Kalogerakis, E. Learned-Miller, Multi-view Convolutional Neural Networks for 3D Shape Recognition, in: 2015 IEEE International Conference on Computer Vision (ICCV), IEEE, 2015, pp. 945–953.
- [4] A. Boulch, B. L. Saux, N. Audebert, Unstructured Point Cloud Semantic Labeling Using Deep Segmentation Networks, in: I. Pratikakis, F. Dupont, M. Ovsjanikov (Eds.), Eurographics Workshop on 3D Object Retrieval, The Eurographics Association, 2017.
- [5] J. Guerry, A. Boulch, B. L. Saux, J. Moras, A. Plyer, D. Filliat, SnapNet-R: Consistent 3D Multi-view Semantic Labeling for Robotics, in: 2017 IEEE International Conference on Computer Vision Workshops (ICCVW), IEEE, 2017, pp. 669–678.
- [6] A. Dai, M. Nießner, 3DMV: Joint 3D-Multi-view Prediction for 3D Semantic Scene Segmentation, in: V. Ferrari, M. Hebert, C. Sminchisescu, Y. Weiss (Eds.), Computer Vision – ECCV 2018, Springer International Publishing, Cham, 2018, pp. 458–474.
- [7] D. Maturana, S. Scherer, VoxNet: A 3D Convolutional Neural Network for real-time object recognition, in: IEEE International Conference on Intelligent Robots and Systems, Vol. 2015-Decem, 2015, pp. 922–928.
- [8] Z. Wu, S. Song, A. Khosla, F. Yu, L. Zhang, X. Tang, J. Xiao, 3D ShapeNets: A deep representation for volumetric shapes, in: Proceedings of

the IEEE Computer Society Conference on Computer Vision and Pattern Recognition, Vol. 07-12-June, IEEE, 2015, pp. 1912–1920.

- [9] C. R. Qi, H. Su, M. Niessner, A. Dai, M. Yan, L. J. Guibas, Volumetric and Multi-View CNNs for Object Classification on 3D Data, 2016 IEEE Conference on Computer Vision and Pattern Recognition (CVPR) (2016) 5648–5656.
- [10] A. Dai, A. X. Chang, M. Savva, M. Halber, T. Funkhouser, M. Nießner, ScanNet: Richly-annotated 3D reconstructions of indoor scenes, in: Proceedings - 30th IEEE Conference on Computer Vision and Pattern Recognition, CVPR 2017, Vol. 2017-Janua, IEEE, 2017, pp. 2432–2443.
- [11] L. Tchapmi, C. Choy, I. Armeni, J. Gwak, S. Savarese, SEGCloud: Semantic segmentation of 3D point clouds, in: Proceedings - 2017 International Conference on 3D Vision, 3DV 2017, 2017, pp. 537–547.
- [12] M. Tatarchenko, A. Dosovitskiy, T. Brox, Octree Generating Networks: Efficient Convolutional Architectures for High-resolution 3D Outputs, in: Proceedings of the IEEE International Conference on Computer Vision, Vol. 2017-Octob, IEEE, 2017, pp. 2107–2115.
- [13] F. Scarselli, M. Gori, Ah Chung Tsoi, M. Hagenbuchner, G. Monfardini, The Graph Neural Network Model, IEEE Transactions on Neural Networks 20 (1) (2009) 61–80.
- [14] X. Qi, R. Liao, J. Jia, S. Fidler, R. Urtasun, 3D Graph Neural Networks for RGBD Semantic Segmentation, in: 2017 IEEE International Conference on Computer Vision (ICCV), IEEE, 2017, pp. 5209–5218.
- [15] T. N. Kipf, M. Welling, Semi-Supervised Classification with Graph Convolutional Networks, in: International Conference on Learning Representations (ICLR), 2017.

- [16] Y. Wang, Y. Sun, Z. Liu, S. E. Sarma, M. M. Bronstein, J. M. Solomon, Dynamic Graph CNN for Learning on Point Clouds, *ACM Transactions on Graphics (TOG)*.
- [17] N. Verma, E. Boyer, J. Verbeek, FeaStNet: Feature-Steered Graph Convolutions for 3D Shape Analysis, in: *CVPR 2018*, 2018.
- [18] A. Mosella-Montoro, J. Ruiz-Hidalgo, Residual Attention Graph Convolutional Network for Geometric 3D Scene Classification, in: *International Conference on Computer Vision Workshop (ICCVW)*, IEEE, 2019, pp. 4123–4132.
- [19] M. Brown, S. Süssstrunk, Multi-spectral SIFT for scene category recognition, in: *Conference on Computer Vision and Pattern Recognition (CVPR)*, 2011, pp. 177–184.
- [20] L. Xie, F. Lee, L. Liu, Z. Yin, Y. Yan, W. Wang, J. Zhao, Q. Chen, Improved spatial pyramid matching for scene recognition, *Pattern Recognition* 82 (2018) 118–129.
- [21] B. Zhou, A. Lapedriza, A. Khosla, A. Oliva, A. Torralba, Places: A 10 million Image Database for Scene Recognition, *IEEE Transactions on Pattern Analysis and Machine Intelligence*.
- [22] K. Simonyan, A. Zisserman, Very Deep Convolutional Networks for large-scale Image Recognition, *International Conference on Learning Representations*.
- [23] M. George, M. Dixit, G. Zogg, N. Vasconcelos, Semantic Clustering for Robust Fine-Grained Scene Recognition, in: *European Conference on Computer Vision (ECCV)*, Springer International Publishing, 2016, pp. 783–798.
- [24] Y. Li, J. Zhang, Y. Cheng, K. Huang, T. Tan, Df2net: Discriminative feature learning and fusion network for rgb-d indoor scene classification, in: *AAAI*, 2018.

- [25] Z. Cai, L. Shao, RGB-D Scene Classification via Multi-modal Feature Learning, *Cognitive Computation*.
- [26] Y. Li, Z. Zhang, Y. Cheng, L. Wang, T. Tan, MAPNet: Multi-modal attentive pooling network for RGB-D indoor scene classification, *Pattern Recognition* 90 (2019) 436–449.
- [27] D. Du, L. Wang, H. Wang, K. Zhao, G. Wu, Translate-to-Recognize Networks for RGB-D Scene Recognition, in: *Conference on Computer Vision and Pattern Recognition (CVPR)*, IEEE, 2019, pp. 11828–11837.
- [28] S. Gupta, R. Girshick, P. Arbeláez, J. Malik, Learning Rich Features from RGB-D Images for Object Detection and Segmentation, in: *European Conference on Computer Vision (ECCV)*, Springer International Publishing, 2014, pp. 345–360.
- [29] X. Jia, B. De Brabandere, T. Tuytelaars, L. V. Gool, Dynamic Filter Networks, in: D. D. Lee, M. Sugiyama, U. V. Luxburg, I. Guyon, R. Garnett (Eds.), *Advances in Neural Information Processing Systems* 29, Curran Associates, Inc., 2016, pp. 667–675.
- [30] S. Song, S. P. Lichtenberg, J. Xiao, Sun rgb-d: A rgb-d scene understanding benchmark suite, in: *2015 IEEE Conference on Computer Vision and Pattern Recognition (CVPR)*, 2015, pp. 567–576.
- [31] P. K. Nathan Silberman, Derek Hoiem, R. Fergus, Indoor segmentation and support inference from rgb-d images, in: *ECCV*, 2012.
- [32] A. Paszke, S. Gross, S. Chintala, G. Chanan, E. Yang, Z. DeVito, Z. Lin, A. Desmaison, L. Antiga, A. Lerer, Automatic differentiation in pytorch, in: *NIPS-W*, 2017.
- [33] M. Fey, J. E. Lenssen, Fast graph representation learning with PyTorch Geometric, in: *ICLR Workshop on Representation Learning on Graphs and Manifolds*, 2019.

- [34] Y. Cui, M. Jia, T. Lin, Y. Song, S. Belongie, Class-balanced loss based on effective number of samples, in: 2019 IEEE/CVF Conference on Computer Vision and Pattern Recognition (CVPR), 2019, pp. 9260–9269.
- [35] L. Liu, H. Jiang, P. He, W. Chen, X. Liu, J. Gao, J. Han, On the variance of the adaptive learning rate and beyond, in: International Conference on Learning Representations, 2020.